

# Nonlinear Dynamics and Chaos in Third Order Mock Theta Functions

Sai Venkatesh Balasubramanian

*Sree Sai Vidhya Mandhir, Mallasandra, Bengaluru-560109, Karnataka, India.  
saivenkateshbalasubramanian@gmail.com*

---

## Abstract

The present work purports to the generation of a signal based chaos based on Ramanujan's Mock Theta Functions. Specifically, the variable in these functions is viewed as an additively coupled sum of sinusoidal signals, with competing frequencies. Thus, by adapting the seven third order mock theta functions into signals, the derivatives are computed and used to form the corresponding iterative maps, which are studied using phase portraits. It is seen that the phase portraits of three of the seven forms exhibit rich, ornamental patterns, characteristic of chaos. Using these, the bifurcation diagrams are plotted, and the chaotic behavior is quantitatively characterized using Lyapunov Exponent and Kolmogorov Entropy. It is seen that the nature of chaos in the mock theta form based signals indeed depend on the frequency ratio of the driving signals, thus pertaining to a case of signal based chaos, which has the key advantage of easy tunability, which forms the novelty of the present work.

*Keywords:* Chaos Generation, Mock Theta Functions, Frequency Controlled Chaos, Bifurcation Analysis

---

## 1. Introduction

Apart from quantum physics and the theory of relativity, another significant revolution in physics characterizing the past century is the rise of Chaos Theory, with diverse applications including biology, astrophysics, mechanics and information technology [1]-[16]. Characterized by the signatures of determinism and an extreme sensitivity to initial conditions, the heart of Chaos Theory is the mathematical aspect of nonlinearity, as seen by the various iterative maps, nonlinear differential equations and bifurcation analyses seen in literature [1, 2]. The physical implementations of chaos generation, especially in electronics involves the realizations of such nonlinear differential equations using appropriate combinations of op-amps and resistive/capacitive passive components, a circuit typically called the 'Chua Oscillator' [17]-[21]. The resultant chaos generated is a 'system' based chaos, with the initial conditions, and hence control parameters defined as physical parameters, such as resistance or capacitance [17].

In the present work, however, we choose to deviate from this perception, and attempt to generate 'signal' based chaos, with the control parameters as aspects of a signal such as amplitude and frequency. Such a dependence on signal offers the obvious advantage of easy tunability, especially in high frequency Integrated Circuit realizations, often along with simpler realizations exhibiting lesser power dissipation [22, 23]. However, in order to achieve this, sufficient nonlinearity is required, and for this purpose, we consider the Mock Theta Functions, introduced by the Indian mathematician Ramanujan in his last living days [24]-[31]. These functions are typically characterized by sum and product series of a  $q$ -analog variable, with the increasing exponential powers signifying the presence of nonlinearity in the same.

In essence, the mock theta functions, represented in general as  $F(q)$  are viewed as the output signal emerging from a nonlinear system with the driving factor  $q$  represented as an additive coupling of two sinusoidal signals with competing frequencies. Specifically, the seven mock theta functions of order three are considered, and for each case, after representing the function  $F(q)$  as an output signal  $X(t)$ , the time derivative  $X'(t)$  is adopted into a difference equation yielding the corresponding mock theta function iterative map. By studying the evolutionary behavior using phase portraits, the nonlinear dynamics are revealed. It is seen that of the seven functions, three exhibit chaotic dynamics, and for these three, the bifurcation diagrams are plotted, which reveal that the behavior of such systems depend heavily on the parameter  $r$ , which is the frequency ratio between the additively coupled driving sinusoidal signals. The hardware implementation of these three functions are carried out using FPGA, and the nature of chaos dependent on  $r$  is studied using Lyapunov Exponents and Kolmogorov Entropy. The common feature of all the three chaos generating mock theta functions is the sensitive dependence on the frequency ratio, and hence the name 'Frequency Controlled Chaos', with the ensuing ease of tunability forming the novelty of the present work.

## 2. Phase Portraits of the Mock Theta Functions

Ramanujan first mentioned about the mock theta functions in his last letter to Hardy, as 17 functions similar in appearance to Jacobi Theta functions, with the generalized notation  $F(q)$ , where  $|q| < 1$ , which are in essence q-series with exponential singularities [24]-[31]. The mathematician classified the 17 mock theta functions into four of the third order, ten of the fifth order and three of the seventh order, though the precise definition of ‘order’ or ‘mock theta’ has for a long time been elusive [24]-[31].

In the present work, the following steps are performed to adapt a given mock theta function  $F(q)$  into a potential chaos generator.

1. The variable  $q$  is denoted as an additively coupled signal of two sinusoids of frequencies  $f_1$  and  $f_2 = rf_1$ , as

$$q = \sin(2\pi f_1 t) + \sin(2\pi r f_1 t) \tag{1}$$

with  $r$  denoting the ratio between the frequencies, and acting as the key control parameter, as seen later.

2. Using these substitutions,  $f(q)$  is rewritten as a time-varying signal  $X(t)$ , and its time derivative  $X'(t)$  is computed.
3. By discretizing  $X(t)$  and  $X'(t)$  into  $X(i)$  and  $X'(i)$  respectively, a difference equation of the form  $X'(i) = X(i + 1) - X(i)$  is formed.
4. This difference equation is rearranged to give the expression of ‘next’ sample  $X(i + 1)$  in terms of ‘current’ samples  $X(i)$ , as  $X(i + 1) = X(i) + X'(i)$ , this equation termed the ‘Iterative Map’ due to its recurrence nature.
5. The dynamics Iterative Map are studied using the Phase Portrait, which is a plot of  $X'(i)$  in terms of  $X(i)$  for a given  $r$ , illustrating the phase space dynamics and qualitatively serving as a tool to assess various chaotic parameters such as sensitivity and ergodicity. Since  $r$  denotes the frequency ratio of the driving signals, and since the fundamental property of chaos is growing evolutions mismatches, an irrational number such as  $\pi$  is set as the value of  $r$ , in order to maximize the frequency and phase mismatches between the driving signals.
6. The detection of ornamental and rich patterns in a phase portrait is a clear indicator of the presence of chaos in the corresponding mock theta function iterative map. In general, the phase portraits of the seven functions are classified into one of two categories: peaking singularities without richness, and non-peaking behavior with high richness. As will be seen, three of the seven third order mock theta functions exhibit the latter behavior.
7. For such chaotic systems, the bifurcation diagram, plotting the output  $X$  as a function of  $r$  is obtained. This diagram clearly illustrates for what values of  $r$ , the system exhibits chaotic and non-chaotic behavior.

In accordance with the above mentioned procedure, we start with the defined form of the first third order mock theta function  $f(q)$ , given as [24]

$$f(q) = \sum_{n=0}^{\infty} \frac{q^{n^2}}{\prod_{i=1}^n (1 + q^i)^2} \tag{2}$$

By substituting Eq 1 for  $q$ , we obtain the corresponding  $X(t)$ , and the corresponding phase portrait is shown in Fig. (1), for an  $r$  value of  $\pi$ . This phase portrait, as all the others mentioned in this work is obtained from hardware implementation of the  $X(t)$  signals using Altera Cyclone II FPGA. As seen in the plot, this phase portrait consists of a

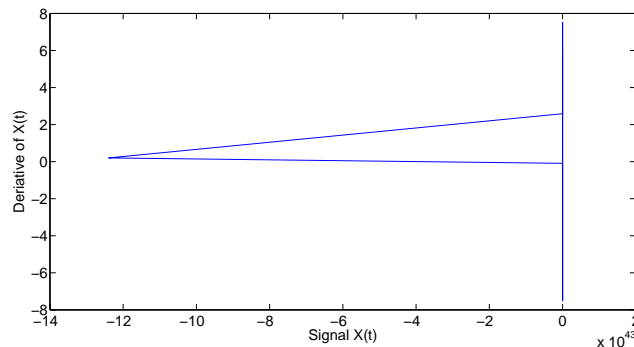


Figure 1: Phase Portrait corresponding to  $f(q)$  with  $r = \pi$

single peak, lacking in sufficient richness to exhibit chaotic behavior.

We now turn towards the second form  $\phi(q)$  given by [24]

$$\phi(q) = \sum_{n=0}^{\infty} \frac{q^{n^2}}{\prod_{i=1}^n (1 + q^{2i})} \quad (3)$$

The corresponding phase portrait is shown in Fig. (2). Unlike the previous case, it is seen that this phase portrait

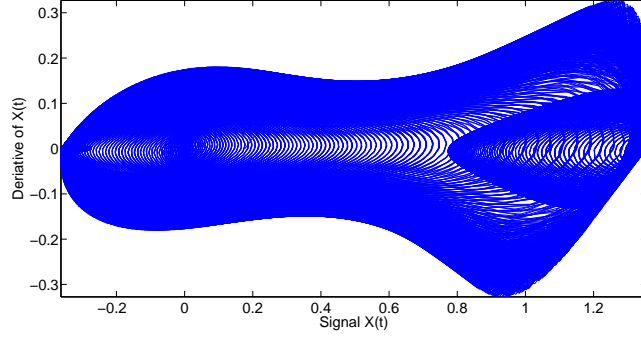


Figure 2: Phase Portrait corresponding to  $\phi(q)$  with  $r = \pi$

exhibits a very rich and ornamental pattern. Thus, this for  $\phi(q)$  is indeed a chaos generating form, and the bifurcation diagram will be plotted in the following section.

The third form  $\psi(q)$  is given as follows, with the corresponding phase portrait in Fig. (3) [24]:

$$\psi(q) = \sum_{n=1}^{\infty} \frac{q^{n^2}}{\prod_{i=1}^n (1 - q^{2i-1})} \quad (4)$$

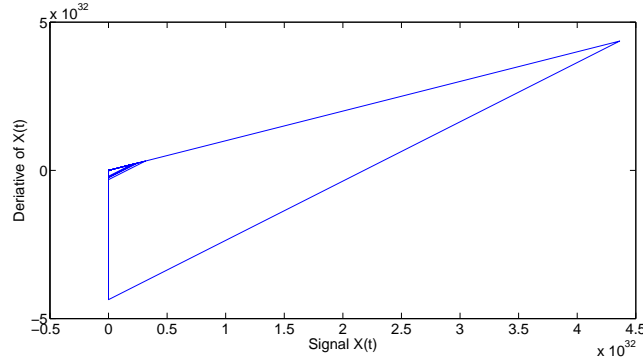


Figure 3: Phase Portrait corresponding to  $\psi(q)$  with  $r = \pi$

This phase portrait too lacks the richness typically characteristic of chaotic systems.

The fourth form  $\chi(q)$  is given as follows, with the corresponding phase portrait in Fig. (4) [24]:

$$\chi(q) = \sum_{n=0}^{\infty} \frac{q^{n^2}}{\prod_{i=1}^n (1 - q^i + q^{2i})} \quad (5)$$

From the phase portrait, it is seen that similar to  $\phi(q)$  the  $\chi(x)$  also exhibits richness characteristic of chaos.

In the same manner, the fifth form  $\omega(q)$  and sixth form  $\nu(q)$ , given as follows are studied using the phase portraits as shown in Fig. (5) and (6) [24].

$$\omega(q) = \sum_{n=0}^{\infty} \frac{q^{2n(n+1)}}{\prod_{i=1}^n (1 - q^{2i+1})^2} \quad (6)$$

$$\nu(q) = \sum_{n=0}^{\infty} \frac{q^{n(n+1)}}{\prod_{i=1}^n (1 + q^{2i+1})} \quad (7)$$

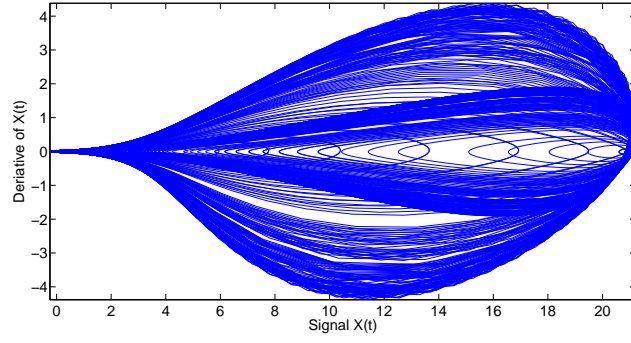


Figure 4: Phase Portrait corresponding to  $\chi(q)$  with  $r = \pi$

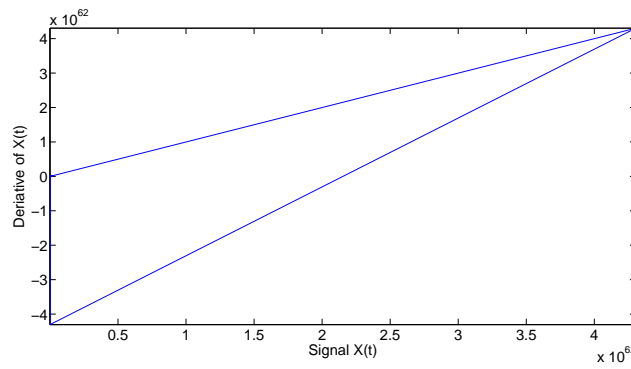


Figure 5: Phase Portrait corresponding to  $\omega(q)$  with  $r = \pi$

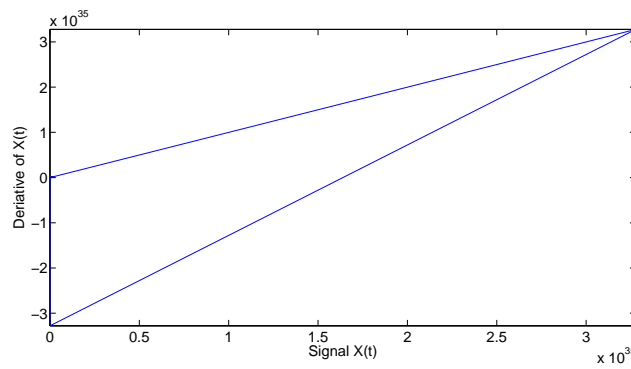


Figure 6: Phase Portrait corresponding to  $\nu(q)$  with  $r = \pi$

As seen from the phase portraits, neither of these forms exhibit richness pertaining to chaos, since both forms are related to peaks with singularities.

Finally, the seventh form  $\rho(q)$  given as follows is plotted as a phase portrait in Fig. (7) [24].

$$\rho(q) = \sum_{n=0}^{\infty} \frac{q^{2n(n+1)}}{\prod_{i=1}^n (1 + q^{2i+1} + q^{4i+2})} \quad (8)$$

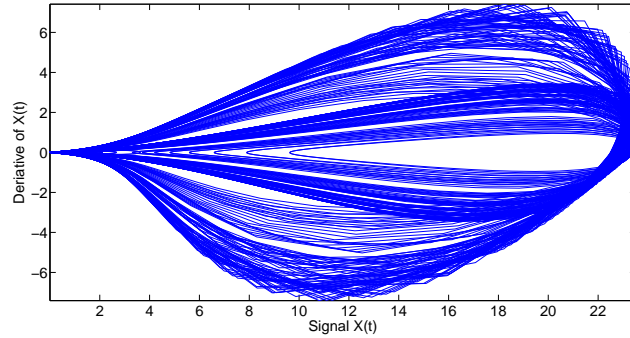


Figure 7: Phase Portrait corresponding to  $\rho(q)$  with  $r = \pi$

As seen from the plot, the  $\rho(q)$  form is also characterized by an ornamental phase portrait.

Thus, in summary, it is seen that three of the seven third order mock theta functions, namely  $\phi(q)$ ,  $\chi(q)$  and  $\rho(q)$  exhibit ornamental phase portrait behavior, characteristic of chaos generating systems. Thus, these forms are selected for subsequent bifurcation analysis.

### 3. Bifurcation Analysis

In this section, the bifurcation analysis for the three chaos generating forms,  $\phi(q)$ ,  $\chi(q)$  and  $\rho(q)$  is presented. It must be noted that, on account of the coupled frequency formation of  $q$  as given in Eq. 1, the three third order mock theta forms do not give rise to bifurcations in the traditional sense; rather they exhibit a quasi-periodic route to chaos, as typically seen in other coupled phase based chaotic systems such as the standard circle map [32]-[37].

Firstly, the  $\phi(q)$  form is considered, where, by substituting  $q$  from Eq. 1, one gets the output signal  $X(t)$ , and from its time derivative, one obtains the following ' $\phi(q)$  Iterative Map':

$$X(i+1) = X(i) + X'_a(i) + X'_b(i) \quad (9)$$

$$X'_a(i) = \frac{2n^2 q^{n^2-1} q'}{QP[-1, q^2, n+1]} \quad (10)$$

$$X'_b(i) = \frac{4q^{n^2} q q'}{QP[-1, q^2, n+1]} \quad (11)$$

where  $QP[a, q, n]$  representing the q-Pochhammer symbol  $(a; q)_n = (a; q)_\infty / (aq^n; q)_\infty$ , given as [24]

$$(aq^n; q)_\infty = \prod_{k=0}^{\infty} (1 - aq^k) \quad (12)$$

The bifurcation diagram corresponding to the  $\phi(q)$  Iterative Map is plotted in Fig. (9). As seen from the plot, the control parameter of the nonlinear behavior is  $r$ , and for certain ratios such as 0.6 and 1.4, dense and grassy patches are seen corresponding to highly chaotic behavior, whereas for certain other values such as 1, quasiperiodic to lowly chaotic behavior is seen. As an example for a non-chaotic ratio, the phase portrait for  $r = 1$  in the  $\phi(q)$  Iterative Map is plotted in Fig (8).

In a similar fashion, the iterative maps of  $\chi(q)$  and  $\rho(q)$  are computed and corresponding bifurcation diagrams are plotted in Fig. (10) and Fig. (11) respectively. It is seen that, similar to  $\phi(q)$  form, the control parameter influencing the transitions from chaotic to non-chaotic regions and vice versa is the frequency ratio  $r$ . However, the chaotic and non-chaotic regions in the three bifurcation plots vary.

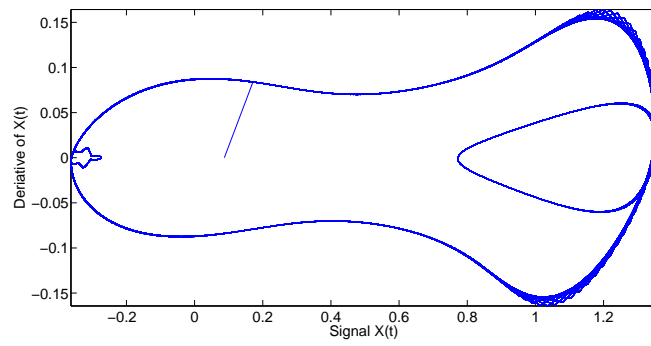


Figure 8: Phase Portrait corresponding to  $\phi(q)$  with  $r = 1$

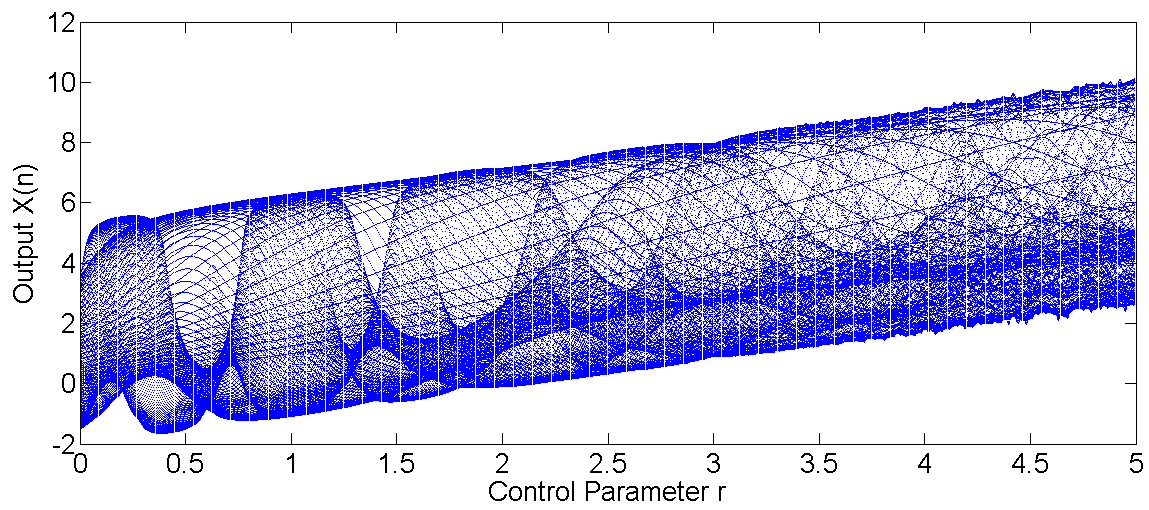


Figure 9: Bifurcation Plot of the  $\phi(q)$  Iterative Map

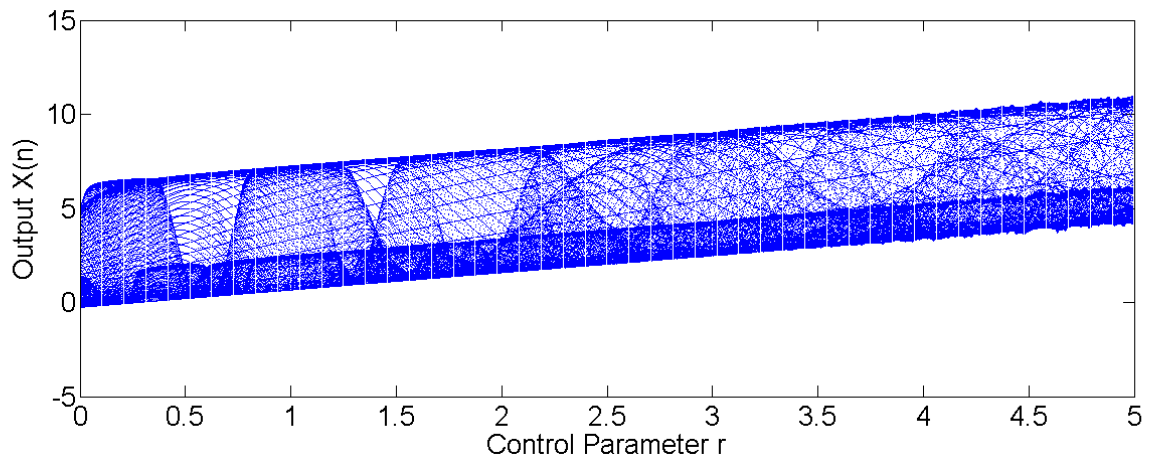


Figure 10: Bifurcation Plot of the  $\chi(q)$  Iterative Map

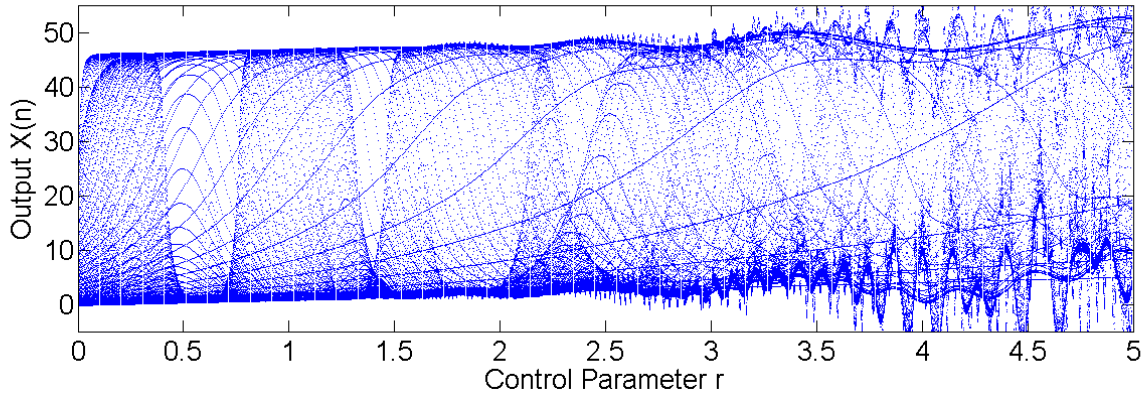


Figure 11: Bifurcation Plot of the  $\rho(q)$  Iterative Map

#### 4. Chaotic Characterization of the $\phi(q)$ , $\chi(q)$ and $\rho(q)$ forms

In order to understand the dependence of the chaotic nature in the generated signals on  $r$ , two well-established chaotic characterization techniques are used:

1. The Largest Lyapunov Exponent (LLE), quantifying the systems sensitive dependence on initial conditions. The Rosensteins algorithm is used to compute the Lyapunov Exponents  $\lambda_i$  from the signal, where the sensitive dependence is characterized by the divergence samples  $d_j(i)$  between nearest trajectories represented by  $j$  given as  $d_j(i) = C_j e^{\lambda_i(i\delta t)}$ ,  $C_j$  being a normalization constant [38, 39].
2. Kolmogorov Entropy, a statistical measure of the uncertainty of the signal. By assigning each of the  $R$  quantifiable states of the amplitude of the output signal as an event  $i$ , the Kolmogorov Entropy  $K$  obtained depends on their probabilities  $p_i$  according to the relation as  $K = - \sum_{i=1}^N p_i \log p_i$ , and is measured in units of nats/symbol [38].

The values of  $K$  and LLE are computed for various values of  $r$  ranging from 1 to 2, and are tabulated in Table 1, for the three forms of  $\phi(q)$ ,  $\chi(q)$  and  $\rho(q)$ .

Table 1: Effect of  $r$  on the nature of output chaos

Form	$\phi(q)$	$\phi(q)$	$\chi(q)$	$\chi(q)$	$\rho(q)$	$\rho(q)$
Ratio $r$	LLE	K	LLE	K	LLE	K
1.0	-0.45	0.67	-0.11	0.87	-0.85	0.54
1.1	0.42	0.69	0.09	0.92	0.79	0.55
1.2	0.48	0.72	0.16	0.94	0.85	0.57
1.3	0.55	0.76	0.26	0.95	0.93	0.59
1.4	1.22	0.82	1.38	0.97	1.12	0.69
1.5	0.75	0.79	0.53	0.93	0.95	0.63
1.6	1.42	0.91	1.36	0.95	0.97	0.67
1.7	1.38	0.86	1.32	0.93	0.96	0.63
1.8	1.35	0.84	1.31	0.91	0.95	0.61
1.9	1.28	0.81	1.27	0.90	0.91	0.59

From the values of  $K$  and LLE in the table, it is seen that while the trends of  $K$  and LLE both are in accordance with the corresponding bifurcation diagrams, the overall ranges for LLE (-0.85 to 1.42) is much higher than  $K$  (0.54 to 0.97), probably owing to the sensitivity aspects of the generated signals.

#### 5. Conclusion

Considering the tunability issues in system based chaos generation circuits such as the Chua Diode, the present work proposes a radically fresh perspective using signal based chaos, and to achieve this, the Ramanujan's Mock Theta Function is considered. Specifically, the seven mock theta functions are adapted into signals by substituting the variable  $q$

as an additively coupled sinusoidal signal, viewing the output as a representative of a nonlinear coupled system. Following this, the derivative of the output is computed and used to form a difference equation, which yields the iterative map of the proposed system. This iterative map is studied using phase portraits, where it is seen that of the seven functions, only  $\phi(q)$ ,  $\chi(q)$  and  $\rho(q)$  exhibit rich ornamental phase portrait patterns characteristic of chaotic systems. Hence, the bifurcation analysis of these three forms are presented following which the dependence of chaotic nature on the frequency ratio  $r$  is studied using Lyapunov Exponents and Kolmogorov Entropy.

Finally, it is noteworthy that since the behavior of the output signal depends on frequency ratio  $r$ , this ratio serves as a secure ‘key’, enabling the use of the Mock Theta Function based Frequency Controlled Chaos in secure communication and encryption systems. The signal oriented approach to generating chaos from mathematical functions, coupled with the easy tunability hence obtained form the novelty of the present work.

## References

- [1] M. Ausloos, M. Dirickx, *The Logistic Map and the Route to Chaos: From the Beginnings to Modern Applications*, (Springer, US, 2006).
- [2] S. H. Strogatz, *Nonlinear Dynamics and Chaos: With Applications to Physics, Biology, Chemistry, and Engineering*, (Westview Press, Cambridge, 2008).
- [3] F. Cramer, *Chaos and Order the Complex Structure of Living Systems*. (Springer, 1993).
- [4] D. S. Coffey, *Self-organization, complexity and chaos: the new biology for medicine*. *Nature medicine* **4**, 882-885 (1998).
- [5] G. Contopoulos, *Order and chaos in dynamical astronomy*, (Springer Science and Business Media, 2002).
- [6] J. Laskar, *Large-scale chaos in the solar system*, *Astronomy and Astrophysics* **287**, L9-L12 (1994).
- [7] A. B. Cambel, *Applied chaos theory-A paradigm for complexity*. (Academic Press, Inc., 1993).
- [8] K. Aihara, *Chaos engineering and its application to parallel distributed processing with chaotic neural networks*. *Proceedings of the IEEE*, **90** 919-930 (2002).
- [9] G. Chen, *Controlling chaos and bifurcations in engineering systems*. (CRC press, 1999).
- [10] R. B. Stull, *An introduction to boundary layer meteorology*. (Springer Science and Business Media, 1988).
- [11] M. F. Barnsley, A. D. Sloan, *Chaotic Compression*, *Computer Graphics World*, **3** (1987).
- [12] K. E. Barner G. R. Arce, *Nonlinear Signal and Image Processing: Theory, Methods, and Applications*, (CRC Press, U.S, 2003).
- [13] S. Saini, J. S. Saini. *Secure communication using memristor based chaotic circuit*. *Parallel, Distributed and Grid Computing (PDGC), 2014 International Conference on*. IEEE, (2014).
- [14] S. Shaerbafe, S. A. Seyedin. *Nonlinear Multiuser Receiver for Optimized Chaos-Based DS-CDMA Systems.*, *Iranian Journal of Electrical and Electronic Engineering* **7**, 149 (2011): 149.
- [15] L. Kocarev, *From chaotic maps to encryption schemes*. *Circuits and Systems*, (1998).
- [16] G. Jakimoski, L. Kocarev. *Chaos and cryptography: block encryption ciphers based on chaotic maps*. *IEEE Transactions on Circuits and Systems I: Fundamental Theory and Applications* **48** 163-169 (2001).
- [17] E. Bilotta and P. Pantano, *A gallery of Chua attractors*, (World Scientific, Singapore, 2008).
- [18] L. Chua, *A universal circuit for studying and generating chaos. I. Routes to chaos*. *Circuits and Systems I: Fundamental Theory and Applications*, *IEEE Transactions on* **40** 732-744 (1993).
- [19] G. Kolumban, M. P. Kennedy, L. O. Chua. *The role of synchronization in digital communications using chaos. II. Chaotic modulation and chaotic synchronization*, *Circuits and Systems I: Fundamental Theory and Applications*, *IEEE Transactions on* **45**, 1129-1140 (1998).
- [20] L. Chua, *Chaos synchronization in Chua's circuit*, *Journal of Circuits, Systems, and Computers* **3**, 93-108 (1993).
- [21] L. Chua, *Experimental chaos synchronization in Chua's circuit*. *International Journal of Bifurcation and Chaos* **2**, 705-708 (1992).
- [22] B. Razavi, *RF Microelectronics*, (Prentice Hall, US, 2011).
- [23] M. Chan, K. Hui, C. Hu, P. K. Ko, *A robust and physical BSIM3 non quasi static transient and AC small signal model for circuit simulation*, *IEEE Transactions on Electron Devices*. **45**, 834 (1998).
- [24] R. Bellman, *A brief introduction to theta functions*, Courier Corporation, (2013).
- [25] K. Bringmann, K. Ono, *The  $f(q)$  mock theta function conjecture and partition ranks*, *Inventiones mathematicae* **165**, 243 (2006).
- [26] G. N. Watson, *The final problem: an account of the mock theta functions* *Journal of the London Mathematical Society*, **1**, 55 (1936).
- [27] S. Zwegers, *Mock Theta-functions and Real Analytic Modular Forms* *Contemp. Math* **291**, 269 (2001).
- [28] D. Zagier, *Ramanujans mock theta functions and their applications* *Astrisque* **326**, 143 (2009).
- [29] W. N. Bailey, *Generalized Hypergeometric Series*, Cambridge Tracts in Mathematics and Mathematical Physics (1935).
- [30] M. Hazewinkel, *Ramanujan function*, *Encyclopedia of Mathematics*, Springer (2001).
- [31] B. C. Berndt, S. S. Huang, J. Sohn, S. H. Son, *Some Theorems on the Rogers-Ramanujan Continued Fraction in Ramanujan's Lost Notebook*, *Trans. Amer. Math. Soc.* **352**, 2157 (2000).
- [32] A. Kudrolli, A. J. P. Gollub. *Patterns and spatiotemporal chaos in parametrically forced surface waves: a systematic survey at large aspect ratio*. *Physica D: Nonlinear Phenomena* **97**, 133-154 (1996).
- [33] J. Briggs, *Fractals: The patterns of chaos: A new aesthetic of art, science, and nature*. (Simon and Schuster, 1992).
- [34] M. Lakshmanan, S. Rajaseekar, *Nonlinear dynamics: integrability, chaos and patterns*. (Springer Science and Business Media, 2012).
- [35] I. R. Epstein, K. Showalter. *Nonlinear chemical dynamics: oscillations, patterns, and chaos*. *The Journal of Physical Chemistry* **100** 13132-13147 (1996).
- [36] R. Gilmore, M. Lefranc, *The Topology of Chaos*, (Wiley, US, [2002]).
- [37] J. M. T. Thompson, H. B. Stewart, *Nonlinear Dynamics and Chaos* (Wiley, UK, [2002]).
- [38] R. G. James, K. Burke, J. P. Crutchfield, *Chaos forgets and remembers: Measuring information creation, destruction, and storage*, *Int. J Bifurcation Chaos*. **378**, 2124 (2014).
- [39] M. T. Rosenstein, J. J. Collins, C. J. De Luca, *A practical method for calculating largest Lyapunov exponents from small data sets*, *Physica D*, **65**, 117, (1993).